

# A 5mm catheter for constant resolution probing in Fourier domain optical coherence endoscopy

Kye-Sung Lee<sup>1</sup>, Lei Wu<sup>2</sup>, Huikai Xie<sup>2</sup>, Olusegun Illegbusi<sup>3</sup>, Marco Costa<sup>4</sup>, and Jannick P. Rolland<sup>1</sup>

<sup>1</sup>CREOL, College of Optics and Photonics, University of Central Florida, 4000 Central Florida Blvd., Orlando FL

<sup>2</sup>Department of Electrical and Computer Engineering, University of Florida, Gainesville, FL

<sup>3</sup>Department of Mechanical, Materials, and Aerospace Engineering, College of Engineering and Computer Science, University of Central Florida, 4000 Central Florida Blvd., Orlando FL

<sup>4</sup>The Cardiovascular Center, University of Florida Health Science Center, Shands Hospital, Jacksonville, FL

## ABSTRACT

A 5mm biophotonic catheter was conceived for optical coherence tomography (OCT) with collimation optics, an axicon lens, and custom design imaging optics, yielding a 360 degree scan aimed at imaging within concave structures such as lung lobes. In OCT a large depth of focus is necessary to image a thick sample with a constant high transverse resolution. There are two approaches to achieving constant lateral resolution in OCT: Dynamic focusing or Bessel beam forming. This paper focuses on imaging with Bessel beams. A Bessel beam can be generated in the sample arm of the OCT interferometer when axicon optics is employed instead of a conventional focusing lens. We present a design for a 5mm catheter that combines an axicon lens with imaging optics and the coupling of a MEMS mirror attached to a micromotor that allow 360 degree scanning with a resolution of about 5 microns across a depth of focus of about 1.2mm.

Keywords: Fourier-domain optical coherence tomography, optical coherence tomography, axicon lens

## 1. Introduction

Optical coherence tomography (OCT) is a highly sensitive biomedical imaging technique that enables high resolution, cross-sectional imaging in biological tissues and other turbid materials.<sup>1</sup> High axial resolution in OCT is realized by use of a broadband light source whereas the lateral resolution is determined by the numerical aperture of the focusing lens. Although a large numerical aperture of a conventional focusing lens in the sample arm of OCT enables high lateral resolution imaging, a small numerical aperture is required to achieve a large depth of focus that allows making a constant transverse resolution image over a long depth range. To overcome this limitation, approaches to creating a high resolution across a large depth of focus is required. Approaches to solving this problem include dynamic focusing<sup>2-7</sup> and Bessel beam formation using axicon lenses.<sup>8</sup> This paper focuses on the later approach.

The long focal depth and narrow focal linewidth of axicons has been used in metrology,<sup>9</sup> and optical trapping of particles.<sup>10</sup> Recently, the use of axicons was tested in time domain optical coherence tomography and researchers demonstrated 10um resolution.<sup>11</sup> Even more recently, axicons were used in Fourier domain optical coherence microscopy, where the illuminating light path was achieved with an axicon and the light was collected via a beam splitter using conventional imaging lenses.<sup>12</sup> Researchers reported 1.5um resolution across a 200um depth of focus.

<sup>1</sup> [kslee@creol.ucf.edu](mailto:kslee@creol.ucf.edu); Phone: 407-823-6853; Fax: 407-823-6880

Endoscopic Microscopy II, edited by Guillermo J. Tearney, Thomas D. Wang  
Proc. of SPIE Vol. 6432, 64320B, (2007) · 1605-7422/07/\$18 · doi: 10.1117/12.711122

In this paper, we present a catheter design for endoscopic Fourier domain optical coherence microscopy (EOCM) which combines OCM with endoscopy. A lens design concept of the catheter was recently presented using a 1mm axicon lens.<sup>13</sup> Miniaturization of optics is a challenge and cost is prohibitive for prototyping. The new contribution of this paper is the investigation of trade-off between depth of focus and beam diameter necessary for miniaturization, the final manufacturable optical design of a 5mm catheter based on a 3mm axicon, and the validation of resolution of the miniature axicon lens. In the remainder of this paper, we present in Section 2 a comparison of imaging between the axicon and two spherical lenses of numerical aperture 0.02 and 0.06, respectively. In Section 3, we present the design of the 5mm catheter for EOCT that incorporates a 3mm diameter axicon with re-imaging optics that together achieve a resolution of about 5 micron across a DOF of about 1.2mm. Finally, we quantify the point spread functions along the depth of focus.

## 2. Comparison between an axicon lens and a spherical lens

In section 2.1 we review theoretical considerations of axicon imaging, specifically the diffraction patterns of annular apertures and how they relate to axicon imaging. We then investigate the relationship of depth of focus versus beam diameter for difference axicon lateral resolutions achieved with different axicon angles. In section 2.2, we investigate the intensity along the line image formed by the axicon as a function of the distance from the axicon and we compare to the intensity of two spherical lenses around their focus point. Also we quantify the lateral resolution of the axicon and two spherical lenses along the same axial range.

### 2.1 Theoretical consideration

Recently axicon optics, optical elements that produce focal segments within a specified range, have attracted considerable interest because of their unusual properties and versatility in practical applications. In diffraction theory, the focal segment is characterized by non diffraction Bessel beams.<sup>14</sup>

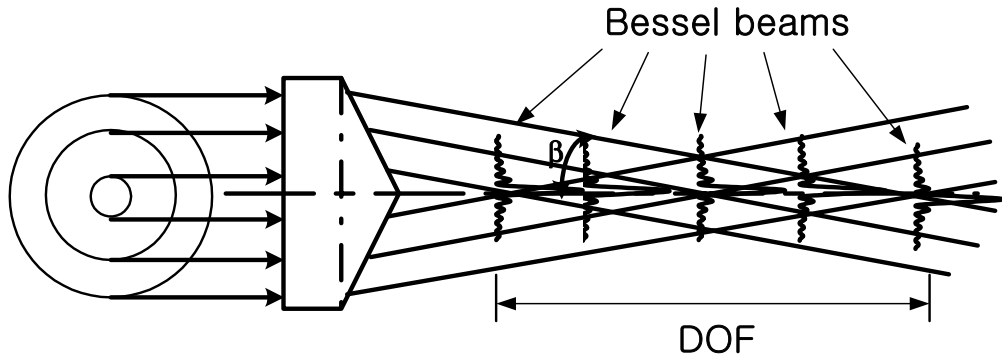


Fig.1 Bessel beams generation with an axicon lens within the focal segment that represents the DOF

Since the  $J_0$  (zero-order Bessel) beam is the Fourier transform of a ring with an infinitively thin width, the conical surface of an axicon generates the diffraction pattern of  $J_0$  beams within the focal segment (i.e. the DOF) as shown in Fig. 1.

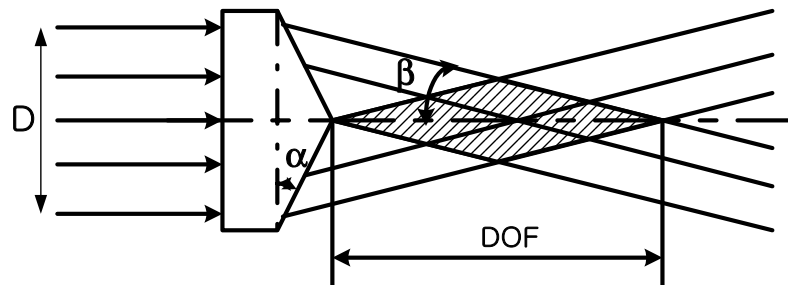


Fig.2. Schematic of an axicon lens

The DOF is defined as the distance from the axicon apex to the geometrical shadow for full-facet illumination, and the DOF is given as

$$DOF = \frac{D \cdot (\cot \beta - \tan \alpha)}{2}, \quad (1)$$

where D denotes the diameter of the collimated incident beam on the axicon lens and  $n$  is the refractive index of the axicon lens. The transverse intensity distribution on each focal plane that is generated from each thin annular segment of the collimated incident beam is described by the first order Bessel function. The central peak radius of the first order Bessel is given by

$$\rho_0 = \frac{2.4048\lambda}{2\pi \sin \beta}, \quad (2)$$

where  $\lambda$  is the central wavelength of the incident beam and  $\beta$  is the beam deviation angle with respect to the optical axis of the axicon lens, shown in Fig. 2, which can be calculated as a function of the axicon angle  $\alpha$  as

$$\beta = \sin^{-1}(n \sin \alpha) - \alpha \quad (3)$$

The central peak radius  $\rho_0$  is constant in the DOF because the beam focusing angle  $\beta$  is also constant within the geometrical shadow as shown in Fig.2. This property yields a constant lateral resolution within the DOF in OCT. Fig. 3 shows a relationship between a geometrical DOF and a beam diameter for each lateral resolution based on Eqs. (1), (2), and (3). A longer DOF can be achieved with a larger beam diameter given some value of lateral resolution. For example, a beam diameter of 0.6mm is needed to get a 3mm geometrical DOF given a 4um lateral resolution.

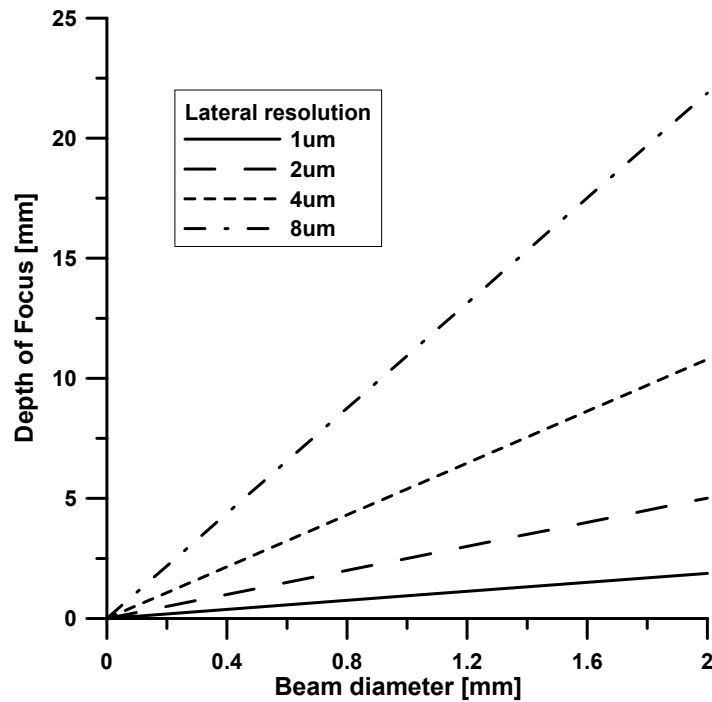


Fig.3 DOF vs. beam diameter for various values of lateral resolution

On the other hand, a conventional lens such as a spherical lens makes a different beam intensity profile width according to the deviation from the nominal focus plane as shown in Fig. 4.

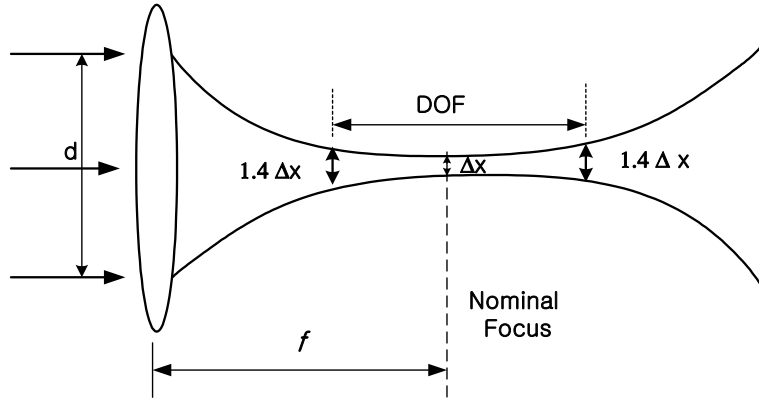


Fig.4 Schematic of a spherical lens

The full width at half maximum  $\Delta x$  of the beam profile at a nominal focus plane of a conventional lens is given by

$$\Delta x = \frac{4\lambda}{\pi} \left( \frac{f}{d} \right) , \quad (4)$$

where  $f$  is the effective focal length of the conventional lens, and  $d$  is the diameter of the collimated incident beam. The DOF shown in Fig. 4 can be described as

$$DOF = \frac{\pi \cdot \Delta x^2}{2\lambda} . \quad (5)$$

Therefore, a high lateral resolution can be achieved around a nominal focus plane by a conventional lens. However the lateral resolutions at deviated planes from the focal plane quickly deteriorate.

## 2.2 Experimental comparison

To compare the on-axis intensity and the lateral resolution as a function of the axial distance between a 25mm spherical lens (NA 0.02), a 8mm spherical lens (NA 0.06), and an axicon lens efficiently in a same chart, the plot for the 25mm spherical lens was shifted to match its focal plane to the focal plane of the 8mm spherical lens in Fig. 5 which shows variations of intensity and lateral resolution for different localization of the detector from the lenses. Fig. 5a demonstrates the trade-off between high intensity and short DOF as obtained with both spherical lenses or the lower intensity and large DOF obtained with the axicon. Fig. 5b clearly demonstrates the much larger depth of field with high lateral resolution of the beam produced by the axicon compared with the two spherical lenses.

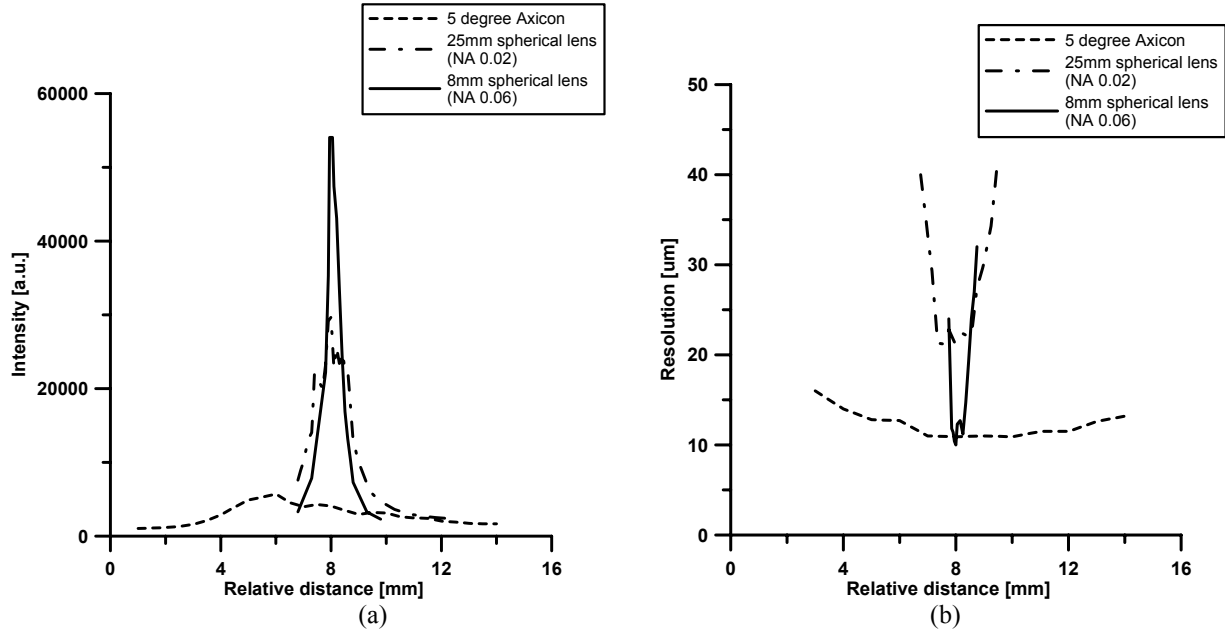


Fig.5 Comparison between axicon and conventional lenses in view of the intensity and resolution along the image depth

### 3. Catheter design

A manufacturable 5 mm biophotonic catheter was conceived to include collimation optics, a 3mm commercial axicon lens, and custom design imaging optics combined with a ~2mm micromotor coupled to a mirror or MEMS to yield a full 360 degree scan within a concave structure such as arteries, lung lobes, and other internal structures. The use of the axicon lens enables around 5 micron across a DOF of about 1.2mm. In Fig 3, although 1mm diameter beam yields about 2.5mm geometrical depth of focus for 5 micron resolution, the point spread functions only within around 1.2mm are distinct due to weak power distribution in the front and rear parts of the geometrical DOF.

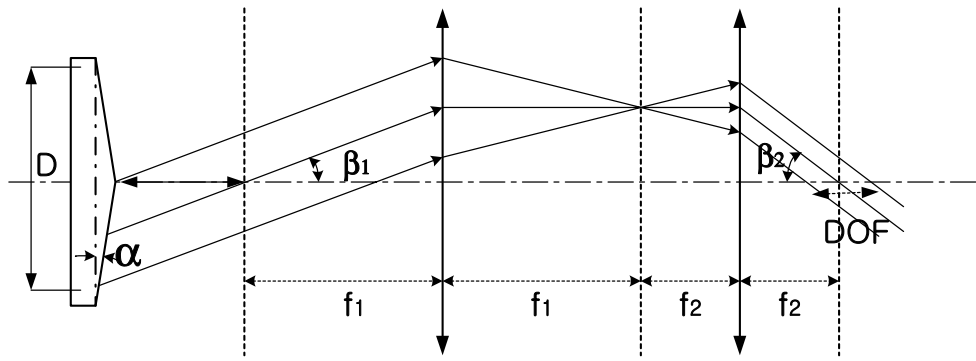


Fig.6 Schematic of a catheter with an axicon and two lenses for relay

Fig. 6 shows the schematic of a catheter with an axicon and two lenses for relay. The axicon has a 5 degrees axicon angle. The effective focal length ( $f_1$ ) of the first lens is 2.4mm and the effective focal length ( $f_2$ ) of the second lens is 1.4mm. The two lenses relay the DOF generated directly from the axicon to the sample area to be imaged. The two lenses also decrease the DOF size by  $(f_1/f_2)^2$  to confine power within a smaller area compared to having no relay lenses,

which yields more power efficiency. In addition, the focusing angle  $\beta_1$  is increased by  $(f_1/f_2)$  to yield  $\beta_2$  which yields higher resolution (i.e. 5  $\mu\text{m}$ ) than before the relay optics, as shown in Fig. 6.

**Table 1** parameters and specifications for the 5mm catheter design

$\alpha$ [degree]	Material of axicon	D [mm]	f1 [mm]	f2 [mm]	DOF [mm]	$\rho_0$ [ $\mu\text{m}$ ]
5	fused silica	1	2.4	1.4	~1.2	~5

With the parameters and specifications for the 5mm catheter design shown in Table 1, we optimized the design. Fig. 7 shows the layout of the 5mm diameter catheter including an optical fiber, a collimating lens, an axicon lens, a singlet lens, and a 1.9mm micromotor coupled to a MEMS mirror/lens with a shaft and a transparent cover. The MEMS mirror/lens device combines a 45°-tilted mirror and an integrated microlens.<sup>15</sup> The microlens turns with the spinning shaft of the micromotor to realize 360° focusing. A lateral resolution of around 5  $\mu\text{m}$  across a DOF of about 1.2mm was achieved. The catheter was designed and optimized at the three different wavelengths of 920nm, 950nm and 980nm with weighting matching the source spectrum. Fig. 8 shows the point spread functions at the focal plane of 0.6mm, 1.2mm, and 1.8mm from point P shown in Fig. 7. The central peak radius of the corresponding point spread functions are 5.5  $\mu\text{m}$ , 5.1  $\mu\text{m}$ , and 4.9  $\mu\text{m}$ .

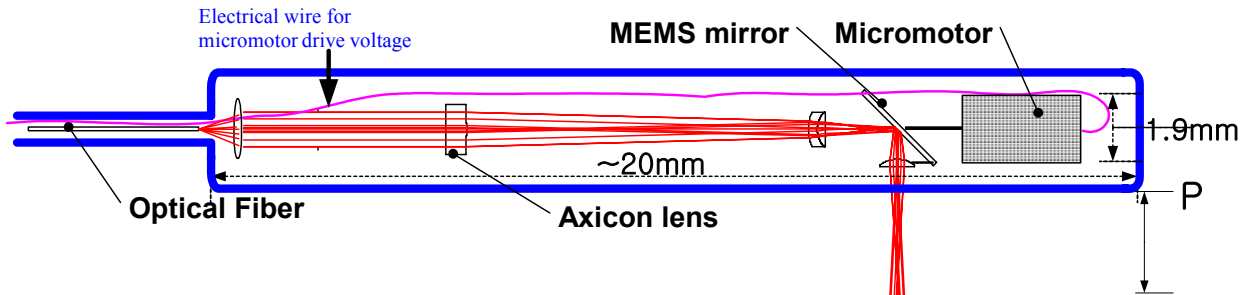


Fig.7 2D layout of a 5mm diameter catheter

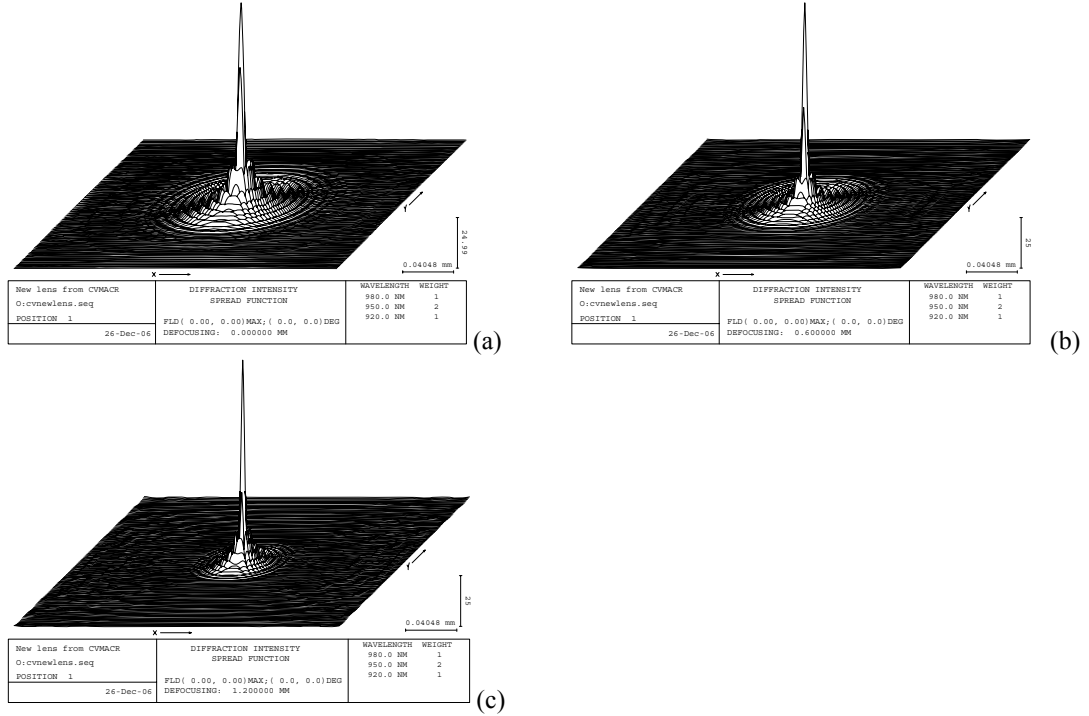


Fig.8 Point spread functions at focal planes of (a) 0.6mm (b) 1.2mm (c) 1.8mm from the point P shown in Fig.7

#### 4. Conclusion and Discussion

In this paper, we presented the design of a 5mm catheter for endoscopic optical coherence microscopy that yields a resolution of around 5 microns across a DOF of about 1.2mm. We demonstrated the impact of an axicon lens on the lateral resolution in OCT compared to a conventional lens. An axicon lens incorporated in OCM can render a constant high lateral resolution over long depths of focus compared to conventional lenses that can image only short depth ranges with high lateral resolution. However higher signal to noise ratio images can be obtained around the focal plane of a spherical lens in OCT because the full beam power is sent to a small area around the focal point while the OCM adapted with an axicon lens yields much of the power being distributed over a long depth of focus. Thus the promise is that an axicon lens coupled with a higher power source will yield both superior resolution and good signal to noise ratio.

#### Acknowledgements

This research was supported in part by the Florida Photonics Center of Excellence, the UCF Presidential Instrumentation Initiative, NSF BES-\*0423557, and the DARPA & NSF PTAP program.

## References

1. D. Huang, E. A. Swanson, C. P. Lin, J. S. Schuman, W. G. Stinson, W. Chang, M. R. Hee, T. Flotte, K. Gregory, C. A. Pulifito, and J. G. Fujimoto, "Optical coherence tomography," *Science* 254, 1178-1181 (1991).
2. W. Drexler, U. Morgner, F. X. Kortner, C. Pitris, S. S. Boppart, X. D. Li, E. P. Ippen, and J. G. Fujimoto, "In vivo ultrahigh-resolution optical coherence tomography," *Optics Letters* 24, 1221-1223 (1999).
3. J.M. Schmitt, S.L. Lee, K.M. Yung, "An optical coherence microscope with enhanced resolving power in thick tissue," *Opt. Comm.*, 142, 203-207, 1997.
4. F. Lexer *et al.*, "Dynamic coherent focus OCT with depth independent transversal resolution," *J. Mod. Opt.*, 46, 541-553, (1999).
5. B. Qi, A.P. Himmer, L.M. Gordon, X.D. Yang, L.D. Dickensheets, I.A. Vitkin, "Dynamic focus control in high-speed optical coherence tomography based on a microelectromechanical mirror," *Optics Comm.*, 232, 123-128, (2004).
6. Divetia *et al.*, "Dynamically focused optical coherence tomography for endoscopic applications," *Appl. Phys. Lett.*, 86, 103902, (2005).
7. S. Murali and J. P. Rolland "Dynamic-focusing Microscope Objective for Optical Coherence Tomography," International Optical Design Conference/SPIE/OSA, Proc. SPIE 6342 (2006).
8. J. H. McLeod, "The axicon: a new type of optical element," *J. Opt. Soc. Am. A* 18, 592-597 (1954).
9. X. Zhang, B. Zhao, and Z. Li, "Measuremet method of spatial straightness error using nondiffracting beam and moiré-fringe technology," *J Opt. A. Pure Appl. Opt.* , 6, 121-126, (2004).
10. J. Arlt, T. Hitomi, and K. Dholakia, "Atom guiding along Laguerre-Gaussian and Bessel light beams," *Appl. Phys. B.* , 71, 549-554, (2000).
11. Zhihua Ding, Hongwu Ren, Yonghua Zhao, J. Stuart Nelson, and Zhongping Chen, "High-resolution optical coherence tomography over a large depth range with an axicon lens," *Optics Letters* 27, 243-245 (2002).
12. R.Leitgeb, M. Villiger, A. H. Bachmann, L. Steinmann, and T. Lasser, "Extended focus depth for Fourier domain optical coherence microscopy," *Optics Letters* 31, 2450-2452 (2006).
13. K. Lee, C. Koehler, E. Johnson, O. Illegbusi and M. Costa, H. Xie and J. P. Rolland "2mm Catheter design for Optical Coherence Microscopy," International Optical Design Conference/SPIE/OSA, Proc. SPIE 6342 (2006).
14. J. Durmin, "Exact solutions for nondiffracting beams," *J. Opt. Soc. Am. A* 4, 651-654 (1987).
15. A. Jain, and H. Xie, "An Electrothermal Microlens Scanner with Low-Voltage, Large-Vertical-Displacement Actuation," *IEEE Photonics Technology Letters*, Vol. 17, No. 9, pp. 1971-1973, September (2005).